Comparison of dynamic characteristics of active sensing methods of Ionic Polymer Metal Composite (IPMC)

Mohdisa, Wanhasbullah; Hunt, Andres; Hosseinnia, S. Hassan

DOI
10.1117/12.2558491

Publication date
2020

Document Version
Final published version

Published in
Electroactive Polymer Actuators and Devices (EAPAD) XXII

Comparison of dynamic characteristics of active sensing methods of Ionic Polymer Metal Composite (IPMC)

MohdIsa, WanHasbullah, Hunt, Andres, HosseinNia, S. Hassan

WanHasbullah MohdIsa, Andres Hunt, S. Hassan HosseinNia, "Comparison of dynamic characteristics of active sensing methods of Ionic Polymer Metal Composite (IPMC)," Proc. SPIE 11375, Electroactive Polymer Actuators and Devices (EAPAD) XXII, 1137519 (19 May 2020); doi: 10.1117/12.2558491

SPIE.

Event: SPIE Smart Structures + Nondestructive Evaluation, 2020, Online Only, California, United States

Comparison of dynamic characteristics of active sensing methods of Ionic Polymer Metal Composite (IPMC)

WanHasbullah MohdIsa[a,b], Andres Hunt[a], and S. Hassan HosseinNia[a]

[a]Department of Precision and Microsytems Engineering, Faculty of Mechanical, Maritime and Materials Engineering, Delft University of Technology, 2628 CD Delft, The Netherlands
[b]Faculty of Manufacturing and Mechatronic Engineering Technology, Universiti Malaysia Pahang, 26600, Pekan, Pahang, Malaysia

ABSTRACT

Limitations of conventional actuators and sensors in small-scaled and complex devices have diverted the researches' attentions towards smart material transducers such as ionic polymer-metal composites (IPMCs). In addition to actuation capabilities, IPMCs generate voltage when subjected to mechanical deformation. Utilization of IPMCs as sensors has been studied much less than IPMC actuation, and direct comparison of sensing methods is required for efficient implementation. This paper characterizes IPMC active sensing methods i.e. voltage, current, and charge in terms of frequency responses, coherence, noise, and repeatability. IPMC is excited mechanically between 0.08 Hz and 60 Hz under identical experimental conditions, while signal and displacement are measured. The results provide an absolute comparison for IPMC active sensing dynamic methods, for a typical IPMC (Nafion, Pt, Na^+).

Keywords: IPMC, sensing, active, method, transducer, ionic polymer, electroactive polymer, smart material

1. INTRODUCTION

Future mechatronics will need to enable applications such as bio-medical instrumentation, micro-fluidic devices, and bio-inspired robots that require increasingly complex and small-scaled designs with embedded sensors and actuators.[1] Therefore, we need suitable transducers both actuation and sensing.[2] Ionic polymer-metal composites (IPMCs) are are smart material transducers that can meet the needs of many of such applications. They are miniaturisable, mechanically compliant, simple in structure, easy to scale, easy to shape, and easy to embed into complex systems, as opposed to bulky and complex conventional transducers.[3,4] IPMCs bend under low voltage stimuli (actuation), and generate electric energy (and variations in impedances) when bent (sensing).[5] The structure of an IPMC comprises ion conducting polymer such as Nafion, sandwiched between two metal electrodes, most commonly platinum, palladium, gold, and silver.[6] Typically it is cut into thin rectangular plate shape.[7]

While IPMC actuation has been widely studied, IPMC sensing has received much less attention.[8] Since the discovery of IPMC sensing capabilities in 1992,[9] sensing has been studied to either understand underlying physical processes,[10–12] investigate characteristics of particular sensing methods,[5,13,14] or propose it for specific application. For example, IPMC has been proposed for seismic,[15] force,[16] multi DOFs-position,[17] vibration,[18] bio-acoustic,[19] pressure,[20,21] flow,[22] and tactile[23] sensors. IPMC sensing methods can be categorized them as: (1) Active methods base on uneven charge re-distribution across the polymer's thickness, creating potential differences between IPMC electrodes, as illustrated in Fig. 1;[5,11,24–29] and (2) Passive methods rely on impedance change of IPMC.[13,30,31] This work focuses on active sensing methods.

IPMC active sensing methods measure either voltage,[5,24–26,32] current,[11,18,24,27,28,33] or charge[20,24,34,35] between IPMC electrodes. Previous studies that report dynamic characteristics of these sensing methods vary

Further author information: (Send correspondence to W.M)
W.M: E-mail: w.h.b.mohdisa@tudelft.nl or wanhasbullah@ump.edu.my
A. H.: E-mail: A.Hunt-1@tudelft.nl
S. H. H.: E-mail: S.H.HosseinNiaKani@tudelft.nl

Electroactive Polymer Actuators and Devices (EAPAD) XXII, edited by Yoseph Bar-Cohen, Iain A. Anderson, Herbert R. Shea, Proc. of SPIE Vol. 11375, 1137519 · © 2020 SPIE · CCC code: 0277-786X/20/$21 · doi: 10.1117/12.2558491

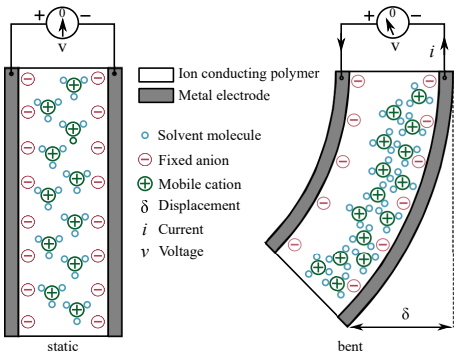

Figure 1. Charge re-distribution within the IPMC polymer generating potential difference across its thickness when bent.

in terms of used materials, displacement stimuli, frequency ranges, and experiment conditions. Responses of IPMC active sensing are well known to significantly depend on these parameters, and therefore absolute comparison between previously reported results is not useful. However, such comparison is required for efficient implementation of IPMC sensors in practice.

This work aims to address these gaps by studying the dynamics of IPMC active sensing methods including their repeatability behaviors. It provides an elaborated approach to our previously reported results[36] by more thoroughly investigating repeatability and noisiness of all active sensing methods. First, frequency responses for all sensing methods are measured on the same IPMC sample under identical experiment conditions. This includes same displacement stimulus, same tested frequencies, and same ambient conditions. We further extract the Bode plots, coherences and signal-to-noise ratios (SNRs) for all methods. The results are then analyzed and compared to each other, providing an accurate comparison of IPMC active sensing methods as well as their individual dynamic behaviors. This is expected to be particularly useful in the future for efficiently implementing IPMC for sensing.

2. EXPERIMENTAL SETUP

We construct a mechanical excitation system to provide sinusoidal excitation to IPMC (section 2.1), build signal conditioning circuits to acquire respective signals (section 2.2), and further process them (section 2.3), in order to identify their dynamic behaviors and compare their characteristics.

In all experiments, we use the same typical IPMC sample, i.e. of Nafion polymer coated with platinum electrodes, ion-exchanged into sodium form and using water for solvent. The size of the sample is 7 mm by 30 mm with a thickness of $\sim$ 200 μm. It was manufactured in-house using chemical deposition of metal on polymer.[37]

2.1 Mechanical Excitation System

The mechanical excitation system is built to provide sinusoidal excitations to the IPMC sensor. Its schematic diagram is shown in Fig. 2 and the completed system is depicted in Fig. 3. IPMC excitations are provided by the electromagnetic shaker B&K Type 4801 (D). The shaker is controlled by a PC with Matlab 2017a environment via NI USB 6211 data acquisition board (A), which also acquires the sensing signals. Data acquisition board output is first amplified and converted into current using a custom-made voltage amplifier (B) and further used to drive the shaping amplifier TIRA Type BAA 120 (C). Two Opto NCDT 1420 laser triangulation sensors (G), which are powered by a 24 V power supply (H), measure the displacements in both ends of the IPMC sample. The difference between these displacements gives the IPMC tip displacement.

In order to achieve consistent displacements over the entire experiment frequency range we identify frequency response of mechanical excitation system in Fig. 5 and use its inverse model to cancel out amplitude differences between frequencies. Before compensation the shaker system behaves like a high-pass filter, greatly affecting the low frequencies. With compensation, we are able to consistently excite IPMC with 1.8 mm displacement peak-to-peak amplitude at all frequencies.

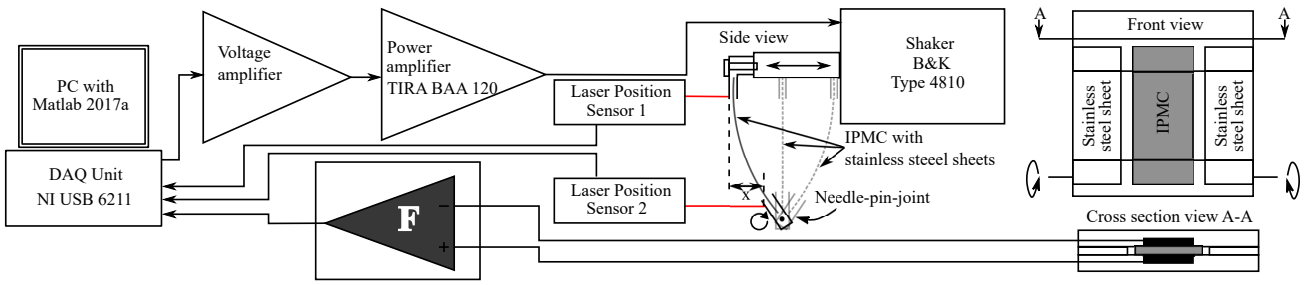

Figure 2. Schematic diagram of the experimental setup. 'F' is metal shielding box, which is equipped with either voltage amplifier ($G = 5.6 \cdot 10^4$), current amplifier ($G = 1.16 \cdot 10^5$) or charge amplifier ($f_c = 15Hz$ and $G_{hf} = 10^{11}$).

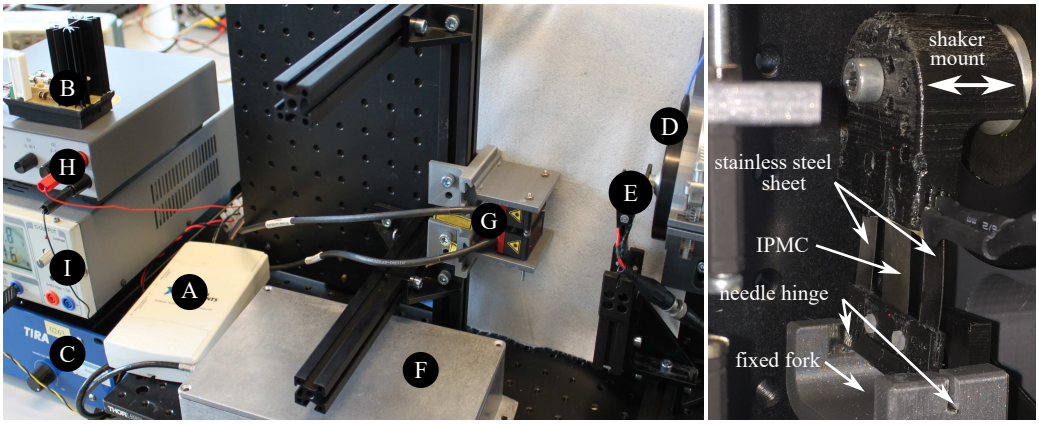

(i) (ii)

Figure 3. Experimental setup. In (i), 'A' is data acquisition board, 'B' is voltage amplifier, 'C' is power amplifier, 'D' is shaker, 'E' is IPMC clamp, 'F' is metal box containing measurement circuit, 'G' is laser triangulation sensors, and 'H' and 'I' are power supplies. (ii) Closed-up photo of the experimental setup 'E'.

In experimental setup we couple the IPMC sample with two stainless steel leaf springs (see Fig. 3 (ii)). This increases the stiffness and thus first resonance frequency of the excitation system, avoiding resonances at investigated frequencies. This condition further restricts the bending of IPMC to only first mode shape. Higher shape modes are avoided, because they consist of reciprocal curvatures on IPMC that cancel out some of the signal. The used leaf springs are 0.10 mm thick and 7 mm wide. The free length of IPMC sample and the springs is 22 mm.

Lower clamp of the IPMC and leaf springs is constrained from moving horizontally using a low-friction pin-in-a-slot joint (see Fig. 3 (ii)). The top clamp is only moved horizontally by the shaker, and therefore the IPMC (and leaf springs) experience only bending with no stretching.

During experiments, IPMC sample is excited at 25 frequencies, logarithmically distributed between 0.08 Hz and 60 Hz. In order to ensure sufficient data for identification, each frequency is applied for at least 5 cycles and 4s. We repeat each experiment five times. All experiments are conducted in open air, where the surrounding temperature is $\sim 23\ ^\circ C$, and relative humidity is 45 %.

2.2 Signal Conditioning Circuits

In this work, we use three signal conditioning circuits in order to measure voltage, current, and charge of IPMC in response to imposed bending. Principle of operation for these circuits are illustrated in Fig. 4. During the experiments, required amplifier is placed in the a metal box 'F' in Fig. 2 and 3 to shield the measured signals from the external interferences.

The first method of IPMC active sensing is measuring voltage between IPMC electrodes. Very high input impedance of the voltage amplifier (see Fig. 4 (i)) ensures no voltage drop due to the measurement.[38] In our work, we use a voltage amplifier with the gain of 56000 V/V.

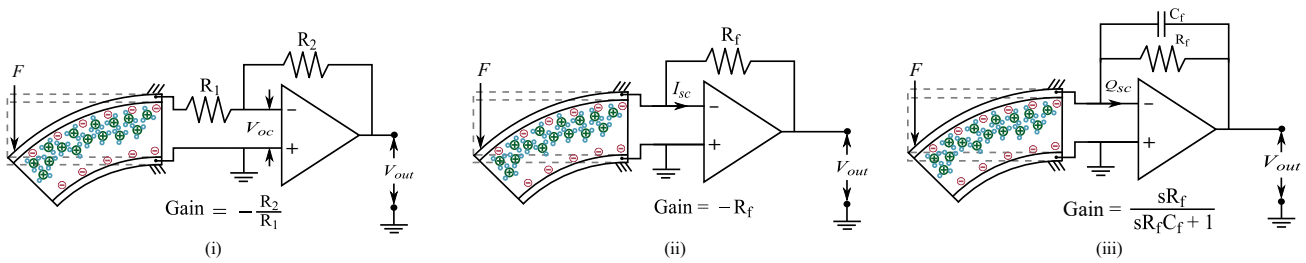

Figure 4. Principle circuit diagrams of the amplifier circuit for IPMC active sensing and their couplings to IPMC.

The second method measures current that's required to maintain zero voltage between IPMC electrodes. The measurement circuit has virtually zero input impedance. In circuit shown in Fig. 4 (ii), the operational amplifier maintains the voltage on its input at zero, and therefore outputs voltage that is proportional to the required current on feedback resistor. Therefore, the circuit converts the current into voltage, and amplifies it.[38] Our two-staged current amplifier has total gain of 116000 V/A.

The third method measures charge generated by the IPMC. For that, IPMC sample is connected to a very low input impedance integrator circuit that operates similarly to current amplifier and converts charge input into voltage output using the circuit shown in Fig. 4 (iii). Due to finite open-loop gain and input offset voltage, a resistor is needed in parallel with the feedback capacitor, resulting in a high-pass filter behavior.[39] We use a two-staged charge amplifier, the resulting cut-off frequency is $15Hz$ and our gain is 10^{11} V/C.

Frequency responses are experimentally measured for all of these circuits and plotted in Fig. 5. They will be further required to convert measurement results back into IPMC voltage, current and charge.

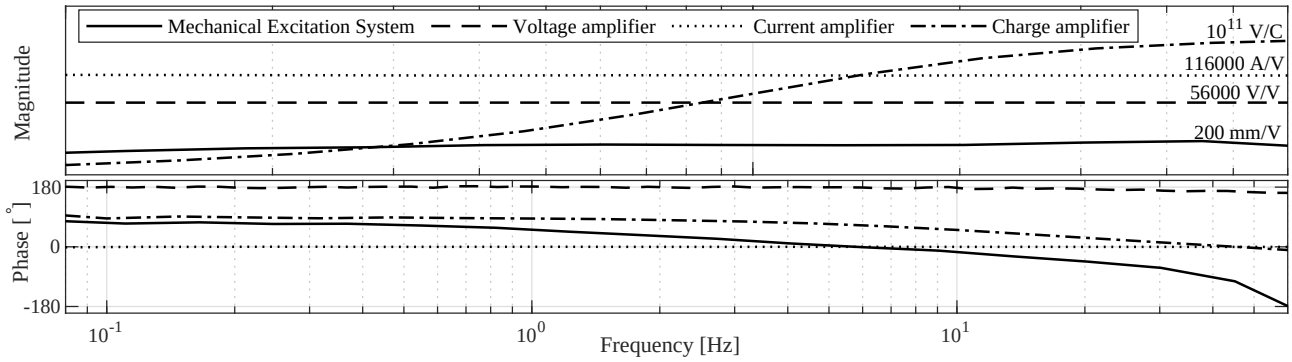

Figure 5. Identified bode plots for parts of our experimental setup: mechanical excitation system, voltage, current, and charge amplifiers.

2.3 Signal Processing

After the experiments, resulting data of each sensing method is further processed to identify their frequency responses, coherences, and signal-to-noise ratios (SNRs). We use 'tfestimate' function in Matlab to obtain all frequency responses from the measurement data. For each frequency, the frequency response component is calculated as follows:

$$TF(\omega) = \frac{P_{sx}(\omega)}{P_{xx}(\omega)} \tag{1}$$

where P_{sx} is the cross power spectral density of IPMC displacement and the sensing signal, and P_{xx} is the power spectral density of IPMC displacement. Coherences are obtained using 'mscohere' function in Matlab, which calculates coherence for each frequency as:

$$C(\omega) = \frac{|\ P_{sx}(\omega)\ |^2}{P_{xx}(\omega) \cdot P_{ss}(\omega)} \tag{2}$$

where P_{xx} and P_{ss} are the power spectral densities of the IPMC displacement and signal respectively. This estimate indicates the linearity between the measured sensing signals and IPMC displacement. In order to obtain SNRs, we first calculate the amplitudes, $A(k)$ of all frequency components, k in the measured signal using fast Fourier transform, calculated by 'fft' function in Matlab:

$$\mathbf{A}(k) = \sum_{n=0}^{N-1} s(n) e^{\frac{-j2\pi kn}{N}} \tag{3}$$

where $s(n)$ is n-th component of the measured signal, $j = \sqrt{-1}$, and N is number of frequency components in the spectrum. SNR is calculated as the quotient between the squared amplitude of the excited signal frequency, A^2_{signal} and mean square amplitude of noise, $\overline{A^2_{noise}}$, both are acquired from Eq. 3. Thus, SNR is calculated as follows:

$$SNR\ [dB] = 10 \cdot log_{10} \frac{A^2_{signal}}{\overline{A^2_{noise}}} \tag{4}$$

Therefore, SNR indicates the strength of the signal's power with respect to the average power of the noise.

3. RESULTS AND DISCUSSION

This section presents and discusses the experimental results based on methodology in section 2. We identify the dynamic characteristics of IPMC active methods i.e. voltage, current, and charge. Before processing, signals on the IPMC electrodes are calculated from the measured signals by using the inverse models of the sensing circuits, identified in Fig. 5. Both average values and standard deviations for all experimental data are calculated to characterize their repeatability.

As shown in Fig. 6, the magnitude in IPMC voltage sensing ranges from several to tens of $\mu V/mm$ and is highly frequency dependent, increasing at +1 slope in logarithmic scale between 0.08 Hz and 1 Hz, at approximately +0.5 slope between 1 Hz and 10 Hz, at approximately +0.25 slope between 10 Hz and 60 Hz. Phase varies between 90° and 180° and roughly increases with frequency. It exhibits good coherence above 0.2 Hz, indicating that voltage relates very linearly to IPMC displacement. SNR in voltage sensing rises with frequency, increasing from ~ 5 dB to ~ 40 dB. Best repeatability i.e. lowest standard deviations is achieved in the middle of our investigated frequency range.

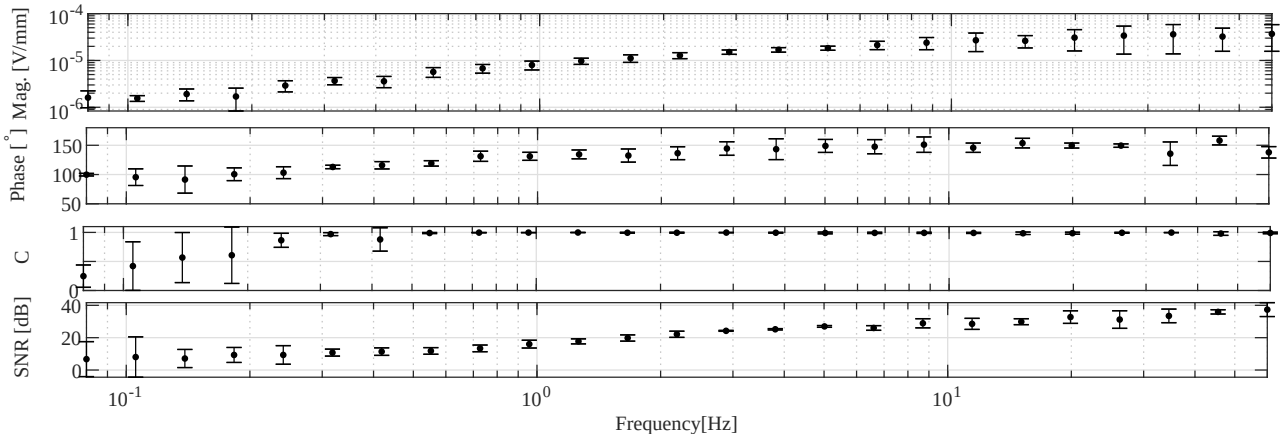

Figure 6. Dynamic characteristics of IPMC voltage.

The results for IPMC current sensing are shown in Fig. 7. Similarly to voltage sensing, the magnitude of IPMC current increases with frequency until approximately 10 Hz. Standard deviations in current sensing are relatively large up to 10 Hz, which is reciprocal behavior to voltage sensing. Phase of current sensing decreases with frequency, remaining between 0° and 90° in our experiments. This method achieves good coherence for frequencies above 1 Hz. Its SNR increases with frequency between 0.08 Hz and ~ 1 Hz to approximately 20 dB, and starts decreasing after 10 Hz.

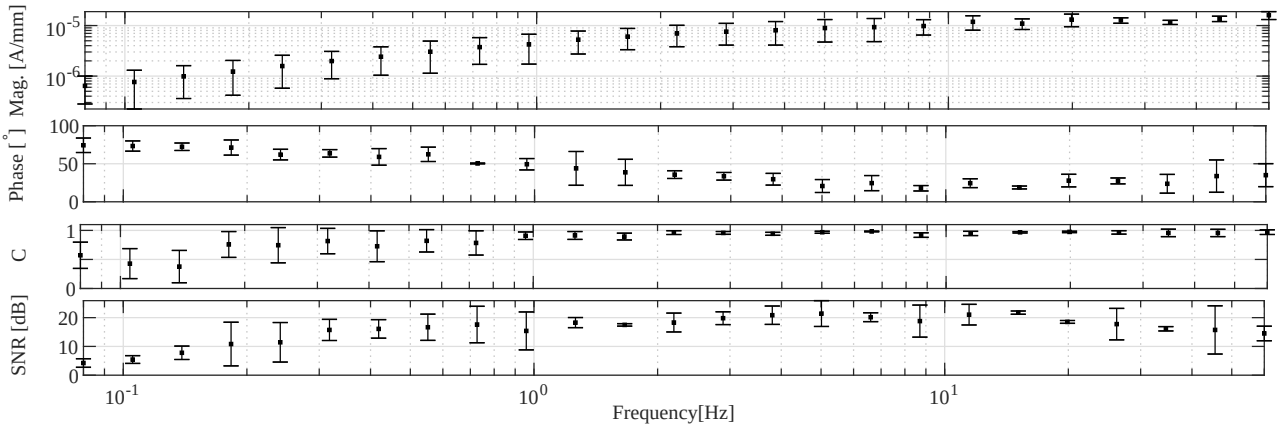

Figure 7. Dynamic characteristics of IPMC current.

Fig. 8 shows results for IPMC charge sensing characterisation. Magnitude and phase of the sensing signal vary without a distinct trend throughout the entire frequency range, with their means remaining between $2 - 20 \cdot 10^{-12}$ C/mm and $-90°$ to $180°$ deg respectively. Coherence and SNR become acceptable at 2 Hz and 1 Hz respectively, meaning that this method is not suitable for quasi-static operation.

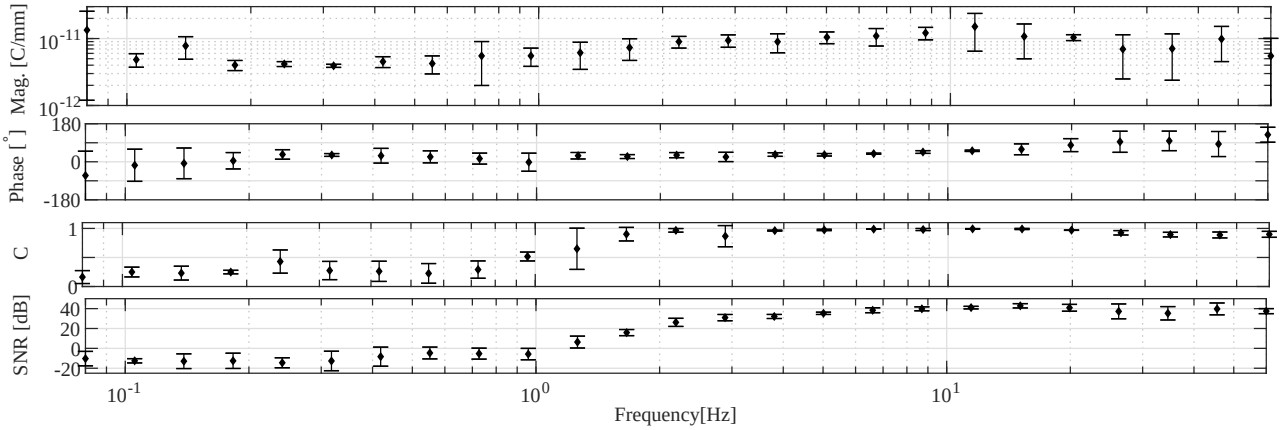

Figure 8. Dynamic characteristics of IPMC charge.

Therefore, IPMC active sensing methods are not suitable for low frequency operation becoming all unusable below 0.2 Hz due to very low coherence and SNR. IPMC voltage sensing is best suited for frequencies between 1 Hz and 10 Hz, and its magnitude standard deviation becomes significantly diverges at higher frequencies. IPMC current sensing is best suited for frequencies above 1 Hz due to its consistently high coherence, acceptable SNR and decreasing standard deviation in the magnitude. IPMC charge sensing is most usable between 2 Hz and 10 Hz. Lower frequencies are limited by poor SNR and cherence, and higher ones by large standard deviation in magnitude reading.

4. CONCLUSION

This paper presents an experimental comparative study of IPMC active sensing methods i.e. measuring IPMC voltage, current, and charge. We experimentally characterize their frequency responses, coherences and signal-to-noise ratios (SNRs). The same IPMC sample is used in all experiments. In all experiments, the IPMC is excited with consistent displacement of 1.8 mm (peak-to-peak) at identical conditions between 0.08 Hz and 60 Hz. IPMC sensing signals are measured using dedicated amplifier circuits, and further processed, analyzed, and compared in frequency domain. The results show that all methods are unsuitable for quasi-static operation

and useless below 0.2 Hz. IPMC voltage sensing is best suited for operation between 0.2 Hz and 10 Hz, IPMC current sensing for frequencies above 1 Hz, and IPMC charge sensing for frequencies between 2 Hz and 10 Hz.

ACKNOWLEDGMENTS

This project has been funded by Malaysia Ministry of Higher Education (MOHE) and University Malaysia Pahang (UMP), Malaysia under Skim Latihan Akademik Bumiputra (SLAB) scholarship program.

REFERENCES

[1] Fry, N., Richardson, R., and Boyle, J. H., [*Integr. Manufact.: The Future of Fabricating Mechatronic Devices*], 129–145, Springer International Publishing (2016).

[2] Bricogne, M., Le Duigou, J., and Eynard, B., [*Design Processes of Mechatronic Systems*], 75–89, Springer International Publishing (2016).

[3] Chen, Z., "A review on robotic fish enabled by ionic polymer–metal composite artificial muscles," *Robotics and Biomimetics* **4**, 24 (Dec 2017).

[4] Hunt, A., Freriks, M., Sasso, L., Esfahani, P. M., and HosseinNia, S. H., "Ipmc kirigami: A distributed actuation concept," in [*2018 Int. Conf. on Manipulation, Automation and Robotics at Small Scales (MARSS)*], 1–6 (July 2018).

[5] Shahinpoor, M., Bar-Cohen, Y., Simpson, J. O., and Smith, J., "Ionic polymer-metal composites (IPMCs) as biomimetic sensors, actuators and artificial muscles - a review," *Smart Mat. Struct.* **7**(6), R15–R30 (1998).

[6] Shahinpoor, M. and Kim, K. J., "Ionic polymer-metal composites: I. fundamentals," *Smart Materials and Structures* **10**(4), 819 (2001).

[7] Palmre, V., Hubbard, J. J., Fleming, M., Pugal, D., Kim, S., Kim, K. J., and Leang, K. K., "An ipmc-enabled bio-inspired bending/twisting fin for underwater applications," *Smart Materials and Structures* **22**(1), 014003 (2013).

[8] MohdIsa, W., Hunt, A., and HosseinNia, S. H., "Sensing and self-sensing actuation methods for ionic polymer–metal composite (ipmc): A review," *Sensors* **19**(18) (2019).

[9] Sadeghipour, K., Salomon, R., and Neogi, S., "Development of a novel electrochemically active membrane and 'smart' material based vibration sensor/damper," *Smart Mat. Struct.* **1**, 172–179 (Jun. 1992).

[10] Nemat-Nasser, S. and Li, J. Y., "Electromechanical response of ionic polymer-metal composites," *J. of Applied Physics* **87**(7), 3321–3331 (2000).

[11] Farinholt, K. and Leo, D. J., "Modeling of electromechanical charge sensing in ionic polymer transducers," *Mechanics of Materials* **36**(5), 421 – 433 (2004). Coupled Chemo-Mechanical Phenomena.

[12] Porfiri, M., "Sensing mechanical deformation via ionic polymer metal composites: A primer," *IEEE Instrumentation Measurement Magazine* **22**, 5–12 (Oct 2019).

[13] Bonomo, C., Fortuna, L., Giannone, P., and Graziani, S., "A method to characterize the deformation of an ipmc sensing membrane," *Sens. and Act. A: Physical* **123-124**, 146 – 154 (2005). Eurosensors XVIII 2004.

[14] Punning, A., Kruusmaa, M., and Aabloo, A., "Surface resistance experiments with ipmc sensors and actuators," *Sensors and Actuators A: Physical* **133**(1), 200 – 209 (2007).

[15] Andò, B., Baglio, S., Beninato, A., Graziani, S., Pagano, F., and Umana, E., "A seismic sensor based on ipmc combined with ferrofluids," *IEEE Trans. on Instr. and Meas.* **62**, 1292–1298 (May 2013).

[16] Liu, L. Q., Chen, Y., Xiang, C. Q., Zhao, Y. S., Hao, L. N., and Zhao, Z. L., "Study on micro-force sensor of cantilever structure based on ipmc," in [*Vehicle, Mechatronics and Information Technologies II*], *Applied Mechanics and Materials* **543**, 1262–1265, Trans Tech Publications (6 2014).

[17] Lei, H., Sharif, M. A., and Tan, X., "Dynamics of omnidirectional IPMC sensor: Experimental characterization and physical modeling," *IEEE/ASME Transactions on Mechatronics* **21**(2), 601–612 (2016).

[18] Paola, B., Fortuna, L., Giannone, P., Graziani, S., and Strazzeri, S., "Ipmcs as vibration sensors," in [*2008 IEEE Instrumentation and Measurement Technology Conference*], 2065–2069 (May 2008).

[19] Griffiths, D. J., *Development of Ionic Polymer Metallic Composites as Sensors*, Master's thesis, Virginia Polytechnic Institute and State University (2008).

[20] Gudarzi, M., Smolinski, P., and Wang, Q.-M., "Bending mode ionic polymer-metal composite (ipmc) pressure sensors," *Measurement* **103**, 250 – 257 (2017).

[21] Gudarzi, M., Smolinski, P., and Wang, Q.-M., "Compression and shear mode ionic polymer-metal composite (ipmc) pressure sensors," *Sensors and Actuators A: Physical* **260**, 99 – 111 (2017).

[22] Lei, H., Sharif, M. A., Paley, D. A., McHenry, M. J., and Tan, X., "Performance improvement of ipmc flow sensors with a biologically-inspired cupula structure," in [*Proc.SPIE*], **9798**, 979827 (2016).

[23] Brunetto, P., Fortuna, L., Giannone, P., Graziani, S., and Strazzeri, S., "A resonant vibrating tactile probe for biomedical applications based on ipmc," in [*2009 IEEE Instrumentation and Measurement Technology Conference*], 658–663, IEEE, Singapore, Singapore (May 2009).

[24] Newbury, K., *Characterization , Modeling , and Control of Ionic Polymer Transducers*, PhD thesis, Virginia Polytechnic Institute and State University, Blacksburg, USA (sep. 2002).

[25] Bonomo, C., Negro, C. D., Fortuna, L., and Graziani, S., "Characterization of ipmc strip sensorial properties: preliminary results," in [*Proceedings of the 2003 International Symposium on Circuits and Systems, 2003. ISCAS '03.*], **4**, IV–IV (May 2003).

[26] Chew, X., Hurk, a. V. D., and Aw, K., "Characterisation of ionic polymer metallic composites as sensors in robotic finger joints," *Int. Journal of Biomechatronics and Biomedical Robotics* **1**(1), 37 – 43 (2009).

[27] Bonomo, C., Fortuna, L., Giannone, P., Graziani, S., and Strazzeri, S., "A resonant force sensor based on ionic polymer metal composites," *Smart Materials and Structures* **17**(1), 015014 (2008).

[28] Lei, H., Lim, C., and Tan, X., "Modeling and inverse compensation of dynamics of base-excited ionic polymer–metal composite sensors," *J. Intel. Mat. Sys. Struct.* **24**(13), 1557–1571 (2013).

[29] Hunt, A., Chen, Z., Tan, X., and Kruusmaa, M., "An integr. electroactive polymer sensor–actuator: design, model-based control, and performance characterization," *Smart Mat. and Struct.* **25**(3), 035016 (2016).

[30] Punning, A., Kruusmaa, M., and Aabloo, A., "A self-sensing ion conducting polymer metal composite (ipmc) actuator," *Sensors and Actuators A: Physical* **136**(2), 656 – 664 (2007). Micromechanics Section of Sensors and Actuators.

[31] Fang, B.-K., Lin, C.-C. K., and Ju, M.-S., "Development of sensing/actuating ionic polymer–metal composite (ipmc) for active guide-wire system," *Sensors and Actuators A: Physical* **158**(1), 1 – 9 (2010).

[32] Zhu, Z., Horiuchi, T., Kruusamäe, K., Chang, L., and Asaka, K., "The effect of ambient humidity on the electrical response of ion-migration-based polymer sensor with various cations," *Smart Materials and Structures* **25**(5), 055024 (2016).

[33] Hunt, A., *Application-Oriented Performance Characterization of the Ionic Polymer Transducers (IPTs)*, PhD thesis, Tallinn University of Technology, Tallinn (april 2017).

[34] Bennett, M. D. and Leo, D. J., "Ionic liquids as stable solvents for ionic polymer transducers," *Sensors and Actuators A: Physical* **115**(1), 79 – 90 (2004).

[35] Griffiths, D., Dominic, J., Akle, B. J., Vlacho, P. P., and Leo, D. J., "Developm. of ionic polymer transducers as flow shear stress sensors: effects of electrode architecture," in [*Proc.SPIE*], **6529**, 65290L (Apr 2007).

[36] MohdIsa, W., Hunt, A., and HosseinNia, S. H., "Active sensing methods of ionic polymer metal composite (ipmc): Comparative study in frequency domain," in [*2019 2nd IEEE International Conference on Soft Robotics (RoboSoft)*], 546–551 (apr 2019).

[37] De Luca, V., Digiamberardino, P., Di Pasquale, G., Graziani, S., Pollicino, A., Umana, E., and Xibilia, M. G., "Ionic electroactive polymer metal composites: Fabricating, modeling, and applications of postsilicon smart devices," *Journal of Polymer Science Part B: Polymer Physics* **51**(9), 699–734 (2013).

[38] Eston, R., Reilly, T., and Reilly, T., [*Kinanthropometry and Exercise Physiology Laboratory Manual: Tests, Procedures and Data: Volume Two: Physiology*], Taylor & Francis (2013).

[39] Rizzoni, G., [*Principles and Applications of Electrical Engineering*], McGraw-Hill Higher Education (2004).